Fracture 1977, Volume 2, ICF4, Waterloo, Canada, June 19 - 24, 1977

HYDROGEN EFFECTS ON FRACTURE OF PH 13-8 Mo STEEL

Anthony W. Thompson*

INTRODUCTION

There are relatively few high-strength steels which have appreciable corrosion resistance; most of these are of the martensitic PH ("precipitation hardenable") type. These steels air harden to form martensite, which can then be further strengthened by heat treatment to form Fe-Ni-Al precipitates. An important aspect of the corrosion behavior of the PH steels is resistance to hydrogen generated by the corrosion reaction. At least some steels of this type, such as 17-7 PH, are severely embrittled by hydrogen [1, 2]. There is, however, relatively little information on either the hydrogen fracture characteristics or on the relation of the fracture to the microstructure. This study was undertaken to examine fracture behavior; a steel widely used in fasteners for modern aircraft, PH 13-8 Mo, was chosen.

EXPERIMENTAL PROCEDURE

The PH 13-8 Mo (trade name of Armco Steel Corp.) steel was acquired in the form of aircraft quality bolt stock, 12.7 mm diameter. The composition was within the specification for the alloy (nominal 13% Cr, 8% Ni, 2% Mo, 1% Al, 0.04% C, 0.1% Mn, 0.05% Si, balance Fe). The steel had been heat-treated to a high-strength condition, about 1500 MPa yield strength, by cold finishing in the solution-treated condition and then aging 4 h at 785 K.

Two types of specimens were tested. One was a conventional tensile specimen with gage section 3.8 mm diameter and 27 mm long. The other was a sharply-notched bar, 60° included angle, with 12.7 mm gross diameter, 3.8 mm net diameter, and 38 μm notch root radius (notch factor $K_t \simeq 15$). Notched bars were tested in either the as-machined condition or after cathodic hydrogen charging. Charging employed 1 N H_2SO_4 saturated with CS_2 for 1 h at room temperature at 0.1mA/mm^2. Upon completion of charging, the material was passivated in 50 vol.% HNO_3 for 0.5 h, a treatment which was found to greatly retard hydrogen evolution. Tensile testing was conducted within 0.5 h of passivation.

Microstructure of the steel was examined using light and transmission electron microscopy. Fracture surfaces were examined at normal incidence in a scanning electron microscope.

* Science Center, Rockwell International, Thousand Oaks, California 91360, U. S. A.

MS128

RESULTS AND DISCUSSION

At the magnifications available in light microscopy, the martensitic structure of the material was apparent; at higher magnifications in thin foils, additional details were evident (Figure 1). The mechanical properties were as follows: yield strength, 1520 MPa ultimate tensile strength (UTS), 1565 MPa reduction of area (RA), 52%. The notch strength was 1.34 times UTS, an indication of the good toughness of this material at a rather high strength level. Regarding these bars as cracked round bars would permit calculation of K_c values [3]; as discussed below, this is regarded as a reasonable procedure for the hydrogen cracking and also in view of recent results on sharp notches [4]. Then the observed abrupt failure load for uncharged material corresponds to a K_c value of 117.3 $MPa\sqrt{m}$. The corresponding value for the notched, hydrogen-charged material is K_c = 46.1 $MPa\sqrt{m}$. The ratio of these K values (and of the respective notch strengths) is 0.39. Hydrogen thus affects the effective toughness of the material in a severely adverse way; by comparison, the threshold K for hydrogen-induced delayed failure in high-strength steels such as 4340, D6aC and H-11 is about 0.30 of the K_c in air [5], a similar decrease.

The large K_c value for uncharged materials, in the present size specimens and without a precrack, precludes any possibility that it might be a "valid" toughness value. As is now discussed, however, it appears feasible to consider validity for the hydrogen-charged material. It would be expected from the behavior of high-strength steels that hydrogen would induce subsurface crack initiation [6]. This was observed in the present experiments. Figure 2 shows that near the notch root, a region of essentially complete dimpled rupture was observed (similar to unnotched tensile specimens), while just below this region was a zone almost totally comprising brittle-appearing fracture topography. Since K rises rapidly with crack depth in cracked round bars [4], and increasing K is known to result in increasingly ductile modes of fracture in high-strength steels [7], the brittle region is interpreted as low-K, sub-notch-root crack initiation [6]. This crack then grew both outward (by ductile rupture of the notch root ligament) and inward.

The peak load failure of this specimen, then, was effectively the failure of a cracked round bar. Furthermore, the specimen size meets recommended criteria for toughness testing [3], and the failure load was 0.54 of net section yielding load, taking into account the $\sqrt{3}$ elevation of yield stress at the net section [4]. The value of 46.1 $MPa\sqrt{m}$ can therefore be taken as the fracture toughness of hydrogen-charged PH 13-8 Mo for the present conditions of temperature, strain rate and hydrogen content.

The fracture surface of the uncharged *tensile* specimens was composed almost entirely of ductile dimples, as was mentioned. The uncharged *notched bar* fractures were also predominantly dimpled (Figure 3a), but the area fraction of brittle-appearing areas (determined by systematic point counting) was 0.37. The center of the *hydrogen-charged* notched bar fracture, Figure 3b, contained a still higher area fraction of brittle areas, 0.61. Higher magnification views of each type of surface showed that the character of the ductile and brittle areas was qualitatively identical except for their relative proportion, as illustrated in Figure 4.

Despite the qualitative similarities in fracture appearance with and without hydrogen, however, there is a quantitative difference: the dimple size differs for the two cases. Dimple diameters were measured near the center of the notched bars, using photographs at 2000X to measure about 50 dimples in each case. The mean dimple diameter was reduced by hydrogen,

from 2.89 ± 0.40 μm without hydrogen, to 2.32 ± 0.39 μm with hydrogen (95% confidence limits). Since the standard error of the difference of these mean values is 0.279 μm, the difference is significant at above the 95% level. Nevertheless, this change corresponds to a fairly minor change in ductility properties; for example, the dimple size ratio R is 0.80, which would be expected to reduce the RA by less than 10% [8]. For this material, with a normal RA of 52%, such a reduction would probably not reduce strength properties at all (e.g., notch strength). Thus the loss in notch strength and in K_c cannot be explained by the reduction in dimple size.

Since no new fracture mode is induced by hydrogen, i.e., there is no change of mode, it may be possible to understand the K_c changes caused by hydrogen in terms of the areal fracture of ductile fracture, by assuming that the ductile process is inherently much tougher than the brittle one. Using the ductile ligament model of Dugdale [9], as formulated in equation (32) of Evans, et al [10], K is roughly proportional to a factor $\phi = 1/(1+d/D)^2$, where D = mean diameter of ductile regions, and d = mean spacing of such regions. Comparing the ratios of the properties with and without hydrogen, the observed K ratio is 2.54, while the ϕ ratio is 2.81. Since the markedly different K_c values with and without hydrogen probably resulted in different stress states, and other factors are neglected here [10], this is relatively good agreement, which seems to indicate that the effect of hydrogen can be simple described as a reduction in the extent of ductile fracture.

CONCLUSIONS

Hydrogen charging considerably reduces the toughness of PH 13-8 Mo steel; the reduction in toughness is similar to other high-strength steels. It appears possible to understand this reduction in terms of the change in the relative proportions of ductile and brittle fracture topographies, using a Dugdale ductile ligament model. Further work on the metallurgical origins of these fracture modes and their relative susceptibility to hydrogen seems indicated and is planned.

ACKNOWLEDGEMENTS

I thank A. G. Evans for stimulating discussions, F. B. Mansfeld for conducing the hydrogen charging, J. C. Chesnutt for scanning electron microscopy, and R. A. Spurling, P. Q. Sauers and E. H. Wright for experimental assistance. This work was conducted as part of the Independent Research Program of Rockwell International.

REFERENCES

1. WALTER, R. J. and CHANDLER, W. T., "Effects of High-Pressure Hydrogen on Metals at Ambient Temperature", Report R-7780-1 (Access No. N70-18637), Rocketdyne Div., Rockwell International, Canoga Park, California, February, 1969.
2. THOMPSON, A. W., Met. Trans., 4, 1973, 2819.
3. BROWN, W. F. and SRAWLEY, J. E., "Plane Strain Crack Toughness Testing of High Strength Metallic Materials", (STP 410), A.S.T.M., Philadelphia, 1969, 15.
4. VROMAN, G. A., "Reconsideration of the Cracked Round Bar Specimen", Report 572-K-11, Rocketdyne Division, Rockwell International, Canoga Park, California, April, 1973.

5. STEIGERWALD, E. A. and BENJAMIN, W. D., Met. Trans., 2, 1971, 606.
6. TROIANO, A. R., Trans. A.S.M., 52, 1960, 54.
7. BEACHEM, C. D., Met. Trans., 3, 1972, 437.
8. THOMPSON, A. W., "Effect of Hydrogen on Behavior of Materials", T.M.S.-A.I.M.E., New York, 1976, 467.
9. DUGDALE, D. S., J. Mech. Phys. Solids, 8, 1960, 100.
10. EVANS, A. G., HEUER. A. H. and PORTER, D. G., Fracture 1977, (Editor, D. M. R. Taplin), University of Waterloo Press, 1977, 529.

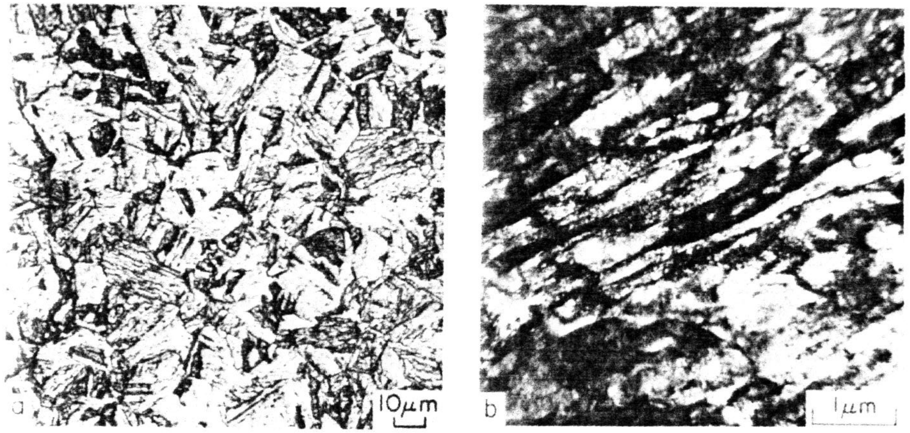

SN 7929, NEG 2144 500X

SN 7929, NEG 33109 TAP 11

Figure 1 Microstructure of PH 13-8 Mo.

(a) Light Micrograph of Polished and Etched Surface
(b) Transmission Electron Micrograph Showing Individual Martensite Laths

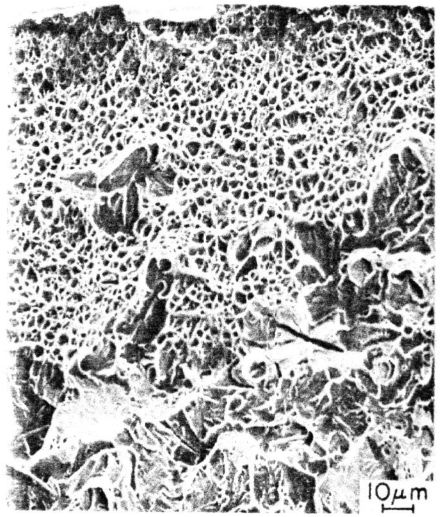

PH 13-8 Mo, Bolt #77/Notch 500 X

Figure 2 Fracture Surface Below Notch Root (Top) in Hydrogen-Charged Specimen. Note Zones of Dimpled (Center) and Brittle (Bottom) Fracture Modes

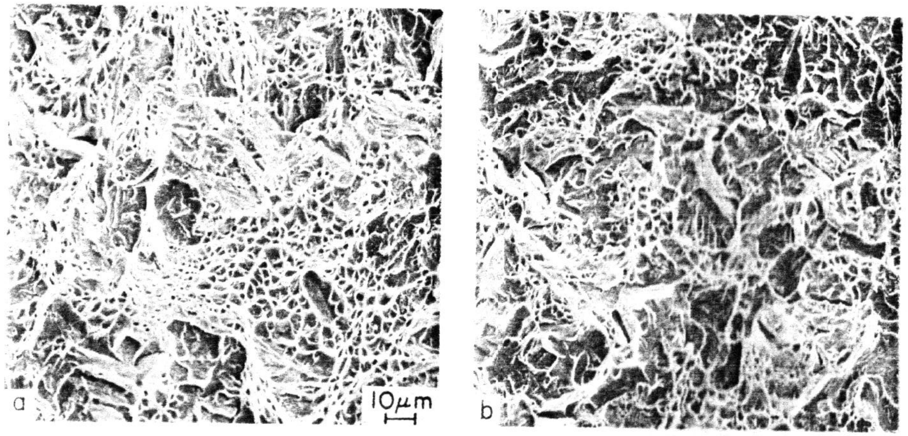

500X

500X

Figure 3 Scanning Electron Micrographs of Fractures in Center of Notched Bars, both at same Magnification

(a) Uncharged
(b) Hydrogen-Charged

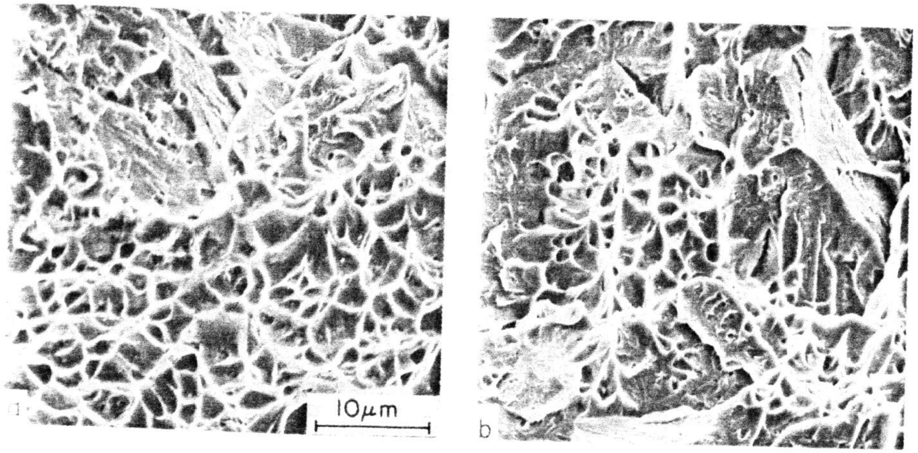

2000X 2000X

Figure 4 Scanning Microscopy of Notched Bar Fractures at Higher Magnification than Figure 3

(a) Uncharged
(b) Hydrogen Charged, Same Magnification as (a)